

The effect of forcing on the spatial structure and spectra of chaotically advected passive scalars

Zoltán Neufeld, Peter H. Haynes and Guillemette Picard

Centre for Atmospheric Science, Department of Applied Mathematics and Theoretical Physics, University of Cambridge,
Silver Street, Cambridge CB3 9EW, UK

(November 18, 2018)

The stationary distribution of passive tracers chaotically advected by a two-dimensional large-scale flow is investigated. The tracer field is forced by resetting the value of the tracer in certain localised regions. This problem is mathematically equivalent to advection in open flows and results in a fractal tracer structure. The spectral exponent of the tracer field is different from that for a passive tracer with the usual additive forcing (the so called Batchelor spectrum) and is related to the fractal dimension of the set of points that have never visited the forcing regions. We illustrate this behaviour by considering a time-periodic flow whose effect is equivalent to a simple two-dimensional area-preserving map. We also show that similar structure in the tracer field is found when the flow is aperiodic in time.

I. INTRODUCTION

It is well known that time-dependent flows with simple spatial structure produce complicated filamental patterns in advected passive scalars through the phenomenon of chaotic advection [1]. Such patterns have been demonstrated in laboratory experiments [2–4] and have also been simulated numerically e.g. [5] (in the context of laboratory experiments) and [6,7] (in the context of the distribution of long-lived chemical species in the atmosphere). Similar structures can be observed in satellite images of oceanic plankton or sea surface temperature [8]. Although the two or three dimensional distribution of atmospheric chemical species is not accessible to high-resolution observations, aircraft measurements along one-dimensional transects give evidence of filaments and irregular structure with strong spatial gradients [6,9,10]. The natural way to characterise these complex spatial distributions is by investigating scaling properties of statistical quantities such as Fourier power spectra or structure functions.

Using concepts from the field of chaotic dynamical systems has proved to be useful in understanding the mechanism of mixing of passive scalars (hereafter we shall use the term ‘tracer’ to describe an advected passive scalar) in fluid flows with a smooth velocity field and has led to the concept of chaotic advection [1] (Lagrangian chaos). It has been recognised that the motion of fluid elements is typically chaotic even in very simple non-turbulent flows. Thus mixing appears as a result of the sensitivity of the particle trajectories to their initial position. By stretching and folding fluid elements chaotic advection generates

finer and finer structures and tracer variance cascades down to small scales until it is dissipated by molecular diffusion and the system ends up in a perfectly mixed homogeneous state.

In order to maintain a nontrivial stationary state it is necessary to apply some kind of forcing in the tracer evolution equation. As we will show in this paper the specific form of this forcing has an important effect on the statistical properties of the resulting tracer distribution.

The usual way to maintain tracer contrast (in numerical experiments and theory) is by a large-scale *additive* forcing representing sources and sinks of the tracer. For this case, theory predicts a power spectrum $\Gamma(k) \sim k^{-1}$ for the tracer [11] - the so called Batchelor spectrum - in the viscous-convective range, that is between the smallest characteristic length scale of the velocity field (L) and the characteristic length scale of diffusion (l_D). Vulpiani has shown [12] that the Batchelor scaling is not restricted to the viscous-convective range of turbulent flows but it is also valid for non-turbulent (e.g. time-periodic) flows if the Lagrangian motion of the fluid elements is chaotic. The k^{-1} spectrum has been verified in recent numerical simulations [13–15]. However, attempts to realise a k^{-1} spectrum in laboratory experiments have been inconclusive [16,17].

In a numerical study [18], Pierrehumbert considered a different type of forcing - a *resetting* forcing - in which, as fluid parcels entered certain localised regions of the flow, tracer concentrations were reset to values associated with the relevant region. This was motivated by giving examples of a number of experimental settings where a *resetting* forcing seems to be more realistic than an *additive* one. Such examples are: *i.*) thermal convection - where the temperature of the fluid parcels is set to the temperature of the hot (lower) or cold (upper) boundary when they cross the thin thermal-boundary layers; *ii.*) advection of dye concentrations - where dye is introduced by diffusion from a solid source and maintained at the saturation concentration in a diffusive boundary layer. We note also that the ‘resetting’ forcing could be relevant for chemical tracers (e.g. ozone or nitrous oxide) in the lower stratosphere, where polar and equatorial regions could play the role of the forcing regions.

In [18] it was found that the power spectrum of the tracer was different from the expected k^{-1} , with spectral exponent between -1 and -2 . However, no precise theoretical explanation for the deviation from the Batchelor spectrum was given.

Tracer spectra steeper than k^{-1} were observed in recent experiments by Williams et al. [17]. The injection of tracer (dye) in these experiments also seems to resemble the 'resetting' forcing.

In this article, we will show that the deviation from the Batchelor spectrum reported in [18] is a direct consequence of the 'resetting' forcing. Using a dynamical system approach we show that this type of forcing leads to the appearance of fractal patterns in the tracer distribution (similar to the ones characteristic of advection in open flows [19,20]) that implies a spectral slope steeper than -1 (and dependent on the fractal dimension of these patterns). In numerical simulations we model advection by a simple two-dimensional area-preserving map representing a time-periodic velocity field. The effect of aperiodicity of the flow is also investigated, by considering a stochastic version of the map.

II. THE MODEL

The tracer concentration field $c(\mathbf{r}, t)$ in an incompressible flow is governed by the equation:

$$\frac{\partial c}{\partial t} + \mathbf{v}(\mathbf{r}, t) \cdot \nabla c = \mathcal{F} + D\Delta c \quad (1)$$

where $\mathbf{v}(\mathbf{r}, t)$ is the velocity field of the flow. We assume that $\mathbf{v}(\mathbf{r}, t)$ is smooth in space with only large scale structure (non-turbulent) and time-dependent. Furthermore, the velocity field is assumed to be independent of the tracer concentration (passive tracers). For simplicity, we will consider two-dimensional flows but we expect that similar considerations apply to large-scale flows in three dimensions. Two-dimensional flows with large scale velocity structure are also relevant for the stratosphere, where the transport is mainly along two-dimensional isentropic surfaces [21,22].

The term \mathcal{F} on the right-hand side of (1) represents the forcing. In case of 'additive' forcing $\mathcal{F} \equiv S(\mathbf{r})$, representing sources ($S > 0$) and sinks ($S < 0$) with a large scale structure. The 'resetting' forcing considered in this paper can be represented mathematically as a limiting case of a relaxation to a concentration profile $c_0(\mathbf{r})$

$$\mathcal{F} \equiv \alpha(\mathbf{r})(c - c_0(\mathbf{r})) \quad (2)$$

where the rate of relaxation $\alpha(\mathbf{r})$ is

$$\alpha(\mathbf{r}) = \begin{cases} \infty & \text{if } \mathbf{r} \in \mathcal{D}_i \\ 0 & \text{otherwise} \end{cases} \quad (3)$$

(The case with constant relaxation rate ($\alpha(\mathbf{r}) \equiv \alpha_0$) representing some kind of homogeneous chemical or biological activity, was investigated in [23,24].) Furthermore we assume, for simplicity, that $c_0(\mathbf{r})$ is constant in each forcing domain, $c_0(\mathbf{r}) \equiv C_i$ for $\mathbf{r} \in \mathcal{D}_i$. Thus the concentration in each fluid element is set to C_i as it enters the

resetting domain \mathcal{D}_i . We will study the properties of the concentration field outside the forcing domains.

We note, that tracer advection in a closed flow with the resetting forcing applied is mathematically equivalent to tracer advection in open flows with time-dependence restricted to a finite mixing region, e.g. in the wake of a cylinder [19,20]. For example, in [20] tracer concentrations were imposed upstream to take one value in part of the inflow and a second, different value on the remainder. The effect of advection through the wake of the cylinder gave a complicated pattern of tracer concentration downstream. In our case, the resetting domains play the role of the upstream condition in the open flow problem, since fluid parcels emerge from those domains with their value of tracer concentration specified. (The resetting domains also mimic the downstream escape in the open flow problem, since when fluid parcels enter those domains their previous value of tracer concentration is immediately forgotten due to the infinitely fast relaxation.) Although in [20] the authors noted that the boundary between different values of tracer concentration had a fractal structure, the implication for the tracer spectrum was not considered.

The second term on the right hand side of (1) represents diffusion, which is assumed to be weak. To make a more precise statement let us denote by τ the characteristic time of the decay in time of the number of fluid particles that have not visited the forcing regions. We assume that the length scale of forcing (L) and the diffusive scale ($l_D \sim (D/\lambda)^{1/2}$) are well separated so that

$$\tau \ll \frac{1}{\lambda} \log \frac{L}{l_D} \quad (4)$$

where λ is the rate at which chaotic advection generates small scale structures, i.e. the absolute value of the most negative Lyapunov exponent of the chaotic advection. (In two-dimensional incompressible flows this is equal to the positive Lyapunov exponent, that is the rate of the exponential separation of nearby fluid elements [1].) The right hand side of (4) is the typical timescale needed for the large scale tracer variance to be dissipated by diffusion [22] that is much larger than the one needed for resetting. Thus, in this case, the fluctuations in tracer structure is primarily affected by the resetting and not by diffusion. Therefore we neglect diffusion in the followings ($D = 0$) but expect to obtain the same structure as it would be for nonzero diffusivity on scales larger than l_D .

In the absence of diffusion the concentration is conserved along the trajectories of fluid elements (except for the resetting) and it is convenient to study the problem (1) in a Lagrangian picture. The concentration for a fluid particle depends only on which resetting domain has last been visited by that particle. Thus, in order to construct the asymptotic tracer distribution we follow the backward trajectories by integrating

$$\frac{d\mathbf{r}}{dt} = \mathbf{v}(\mathbf{r}, t) \quad (5)$$

backwards in time from each point until the trajectory enters one of the resetting domains and assign the concentration corresponding to that domain to the point from where the trajectory started. The concentration distribution along a line segment can be obtained in the same way without having to calculate the whole two-dimensional field. This allows us to reach high resolution easily for one-dimensional transects.

Advection by a two-dimensional incompressible time-periodic velocity field over one time period is equivalent to the action of a two-dimensional area-preserving map. In general, the explicit form of this map cannot be obtained analytically from the velocity field. For numerical convenience, in the detailed analysis of the tracer field that follows we represent advection by a map \mathcal{M} given by,

$$\begin{aligned} x_{n+1} &= x_n + a \sin(2\pi y_n + \phi) \bmod 1, \\ y_{n+1} &= y_n + a \sin(2\pi x_n + \phi) \bmod 1, \end{aligned} \quad (6)$$

where x_n and y_n denotes the coordinates of a fluid particle at discrete times $t = nT$, $n = 0, 1, \dots$ and T is the period of the flow. It is known that the orbits obtained by such iterations are typically chaotic. We note, that the action of the map (6) is equivalent to advection for one period by a piecewise steady flow given by periodic alternation of two sinusoidal shear flows in the x and y direction, respectively.

One characteristic of two-dimensional area-preserving maps is the existence of quasiperiodic orbits that form KAM tori acting as transport barriers [26] separating different chaotic regions of the phase space. In order to avoid such barriers we use a value of the parameter a in (6) that produces a single ergodic chaotic region without visible KAM tori. An alternative approach (used in [18]) is to consider ϕ as a random variable $\phi_n \in [0, 2\pi]$ taking on different values in each step of the iteration. We will first consider the deterministic case ($a = 0.6$, $\phi_n \equiv 0$), and will then discuss the effect of the random parameter, representing aperiodic flows.

Since advection is represented by a map the position of fluid parcels is followed explicitly only at discrete times separated by interval T . We therefore follow Pierrehumbert ([18]) in resetting only at those discrete times and also in considering resetting domains of the form of two parallel stripes of width ϵ . As we shall see later, varying ϵ , and hence the size of the domains, has a strong effect on the resulting tracer distribution. [Note that every specification of the resetting domains in the time-continuous problem defined by (1), with time-periodic flow, (2) and (3), corresponds some resetting domain in the time-discrete problem. The converse, that every resetting domain in the time-discrete problem corresponds to some resetting domain in the time-continuous problem, applies provided the slight generalization is allowed that α is a function of time as well space in the time-continuous problem.]

III. RESULTS AND DISCUSSION

To illustrate the characteristic features of the tracer field forced by 'resetting' we first consider a time-periodic velocity field that is a kinematic model of a meandering jet flow [25]. The resetting domains are taken to be parallel to the mean flow below and above the centre of the jet, respectively. In Fig.1 a snapshot of the concentration field (obtained from the backward iteration described in the previous section) is shown for this meandering jet flow. The periodicity of the flow implies a periodic tracer field for long times. In the absence of barriers outside the forcing regions almost all trajectories visit the forcing regions in a finite time. Thus, the concentration field has only two possible values (C_1 - 'black' and C_2 - 'white'). The tracer field is formed by elongated filaments with a Cantor set like fractal structure transverse to the filaments (see Fig.1b). The width of the filaments varies in a broad range of scales showing that the forcing maintains an imperfectly mixed stationary state. Similar structure can be observed in the tracer field generated by the map (6) (Fig. 2).

The boundary between the two regions of different concentration value is in fact the boundary between the basins of attraction of the two resetting domains for the time-reversed advection dynamics. The structure of boundaries between basins of attraction of different attractors is a well known problem in the field of chaotic dynamical systems [26–28]. Complicated fractal structure of basin boundaries appears as a consequence of non-attracting chaotic sets, usually associated with the phenomenon of transient chaos [29].

Let us consider the set \mathcal{S} of points corresponding to orbits that never visit the forcing domains

$$\mathcal{S} \equiv \{\mathbf{r} | \mathcal{M}^n(\mathbf{r}) \notin \cup_i \mathcal{D}_i, \forall n = -\infty, \infty\}, \quad (7)$$

If the map \mathcal{M} is the same in each iteration the set \mathcal{S} is, by definition, invariant under the iterations of the map, $\mathcal{M}(\mathcal{S}) = \mathcal{S}$. Due to the assumed ergodicity of the advection, \mathcal{S} is necessarily a set of measure zero. Such non-attracting invariant sets in chaotic systems (chaotic saddles) typically have a complex fractal geometry [27,28]. In conclusion, the set of forcing domains selects a subset \mathcal{S} of the existing chaotic trajectories that defines an invariant fractal set.

Fig.3 shows the number of backwards iterations n needed to reach either of the resetting domains from points lying along a line segment. The boundary between the regions with concentration C_1 and C_2 is formed by points for which n is infinite and coincides with the part of the unstable manifold of \mathcal{S} – to be precise the union of the parts of the unstable manifolds of each point in \mathcal{S} that lie between that point and the first resetting domain encountered along the unstable manifold. The results of estimating the fractal dimension D of the boundary along linear transects using the so called box counting algorithm are shown in Fig.4.

For a given flow, the geometry of the resetting regions - by selecting an invariant chaotic set - determine the fractal dimension D . The dependence of D on the size of the resetting stripes ϵ is shown in Fig.5. As the size of the resetting regions increases the fractal dimension of the set corresponding to orbits avoiding these regions decreases. If the resetting domains occupy the whole system, the distribution is formed by a finite number of discontinuities ($D = 0$). (In fact, the fractal dimension D may reach zero even if the forcing domains do not cover the whole chaotic region.) In the limit of very small resetting domains ($\epsilon \rightarrow 0$) the set of orbits avoiding them increases and \mathcal{S} becomes space filling ($D \rightarrow 1$).

The fractal dimension D of the unstable manifold of the chaotic saddle can be related to dynamical properties of the system by a variant of the so called Kaplan-Yorke formula [30] corresponding to non-attracting sets [31]

$$D = 1 - \frac{\kappa}{\lambda}, \quad (8)$$

where λ is the Lyapunov exponent on the chaotic saddle and κ is the escape rate, defined by

$$A(nT) = A_0 e^{-\kappa nT} \quad (9)$$

where $A(nT)$ is the area occupied by points that have not visited the resetting regions by time $t = nT$, ($\kappa \equiv 1/\tau$). In our context κ might more appropriately be called the ‘resetting rate’. (More precisely, (8) gives the so called information dimension [31] D_1 of the invariant measure on the saddle, which can be somewhat smaller than the box counting dimension). If the non-uniformity of the stretching is not too strong the Lyapunov exponent corresponding to any subset of trajectories is close to the Lyapunov exponent of the full advection dynamics. In our case this means that λ has only a weak dependence on ϵ and the fractal dimension depends on the structure of the resetting regions through the ‘resetting rate’ κ .

In general, there is no simple formula for the resetting rate since it depends on the detailed geometry of the resetting domains and the structure of the chaotic trajectories. In the time-discrete version of the problem, however, one can have a situation where mixing is strong enough to redistribute the non-reset particles almost uniformly between two resettings, if $T \gg 1/\lambda$. Then the resetting rate can be approximated by

$$\kappa = -\ln\left(1 - \sum A_i\right), \quad (10)$$

where A_i is the area occupied by the forcing domain i normalised by the area of the whole chaotic region. This approximation seems to apply to our numerical example ($\lambda = 2.75/T$), as is shown in Fig.5, where the fractal dimension of the boundary predicted by (8, 10) is compared with the measurements.

The standard way to characterise such tracer distributions is by their Fourier power spectra. In our case the distribution along a one-dimensional transect is made up

by an infinite number of jumps between the two possible values, with the jumps located on a fractal set (see Fig.2b). The power spectra of such structure has been discussed in [32], and it was found that there is a simple relationship between the spectral slope (γ) and the fractal dimension (D) of the set of the discontinuities

$$\gamma = 2 - D. \quad (11)$$

A more detailed analysis of the relation between fractal dimension and spectral slope in [33] and in [34] (done in the context of advection by compressible flows modelled by dissipative maps with fractal attractors) has shown that D in (11) is the correlation dimension D_2 of the chaotic set. Assuming further that multifractality [35] is weak ($D_2 \approx D_1$) and using (8) the spectral slope can be approximated as

$$\gamma \approx 1 + \frac{\kappa}{\lambda}, \quad (12)$$

where the second term represents the deviation from the Batchelor scaling and is proportional with the rate of ‘resetting’ κ .

For numerical convenience, instead of direct measurement of the power spectra we consider the second order structure function [36] defined by

$$S(r) \equiv \langle (C(r_0 + r) - C(r_0))^2 \rangle \sim (\delta r)^\zeta \quad (13)$$

where $\langle \dots \rangle$ denotes averaging over different values of the coordinate r_0 . The scaling exponent ζ is known to be related to the spectral slope by the simple relationship $\gamma = 1 + \zeta$, if $1 < \gamma < 3$ [37].

Structure functions (calculated for different transects and their average) are shown in Fig.6. Fluctuations of the local slope at large scales decay fast at smaller scales where structure functions calculated from different transects tend to be parallel. This can be explained by the fact that the statistics of the small scale structures is much better (as there are many along a transect) than that of the few large scale features. In this sense, spatial averaging improves the scaling at large or intermediate scales.

The scaling exponent ζ depends on the size of the forcing domains, taking values between $\zeta = 1$, ($\gamma = 2$) and $\zeta = 0$, ($\gamma = 1$). Fig.7 shows the value of ζ as a function of the width, ϵ , of the forcing domains. In order to verify the relationship (11) in our model the measured value of the spectral slope (based on the structure function) is compared with the one predicted from the fractal dimension measurement, for different values of ϵ (Fig.7). The relationship is confirmed with a very good accuracy.

We also performed numerical simulations with the stochastic version of the map (6) representing aperiodic flows. The two-dimensional tracer field (Fig.8) shows a pattern qualitatively similar to the one shown in Fig.2 but with a somewhat less regular character. An obvious difference is that in this case the tracer field changes

with time, although its qualitative appearance remains the same.

In the case of aperiodic flows invariant chaotic sets cannot exist. Nevertheless, there may exist a set of chaotic orbits that never visit the resetting domains. The set of points corresponding to these orbits now wanders from one iteration to the next, but exhibits the same type of fractal structure as seen in the non-random case for the set \mathcal{S} . (The resetting time, when calculated for points lying along one-dimensional transect, also shows a similar structure to that in Fig.3.)

Structure functions for the aperiodic case are shown in Fig.9. As a consequence of aperiodicity, the spatially averaged structure function, measured at fixed time, is now time-dependent. Furthermore, its local slope fluctuates even at relatively small scales. (Compare with Fig.6b.) Nevertheless, the time-average of these structure functions exhibits clear scaling (Fig.9b). (Note, that the slope of the temporally averaged structure function is different from that of the non-random map.) Similar fluctuations of the spectrum have also been observed in the case of attractors of dissipative random maps [34] and in experiments with floating particles advected on the surface of an aperiodic flow [38]. In both cases, temporal averaging led to a good power law scaling.

The lack of good scaling for the spectra taken at fixed times can be explained by the fact that scaling needs a good sampling of the possible stretching histories at each scale. Structures contributing to the spectra at a certain scale l have been advected for a finite time $t_l \sim (1/\lambda) \log(L/l)$. When the flow is aperiodic (i.e the map is different in each time step) the time t_l might not be enough for a good sampling of the possible velocity fields if l is not small enough. This can be compensated by temporal averaging, but obviously cannot be replaced by spatial averaging in this case. We conclude, that for the random map (or aperiodic flows) the power law scaling could be restricted to rather small scales but it is clearly present in the temporally averaged sense. This also holds for the box-counting fractal dimension. There is a well defined fractal dimension in a temporally averaged sense that relates to the exponent of the structure function as in the case of the non-random map.

IV. SUMMARY AND CONCLUSIONS

We have shown that when resetting forcing is applied to a passive tracer in a chaotic advection flow, the boundaries between different tracer values have a fractal structure. Such structure is closely analogous to that previously identified in open flows. As a consequence, when 'resetting' forcing is applied (or, equivalently, when open flows are considered) the spectra is steeper than the k^{-1} predicted by Batchelor for the case of additive tracer forcing. The deviation can be expressed in terms of characteristic exponents of the advection and forcing dynam-

ics. The physical mechanism for the steeper spectra is that most of the tracer variance is destroyed by the resetting forcing (or escape, in open flows) before reaching the dissipative scale. This effect is clearly visible in the tracer distribution (Fig. 2) which contains large smooth regions, while strong gradients (and hence diffusive dissipation rates) are concentrated, in the limit of diffusivity tending to zero, on a fractal set of measure zero

The implication of our results is that the form of the tracer forcing can strongly affect the spectral slope of the advected tracer. Indeed, our results could explain why some previous numerical experiments and most of the previous laboratory experiments have failed to reproduce the k^{-1} spectrum. Our numerical example shows that this is definitely the case for the numerical results presented in [18]. The tracer forcing used in the experiment [17] also seems to be similar to our considerations. Although in [17] the authors try to explain the unexpected deviation from the Batchelor spectra as an intermittency effect, they recognise that the deviation is much stronger than what one would expect for intermittency corrections. This was confirmed recently in [15], where the effect of intermittency (non-uniform stretching) on the spectra was investigated. Non-space-filling, fractal, scalar interface in the Batchelor regime was also detected in jet flows [39] where the open flow type behavior, equivalent to the resetting, should apply. A jet flow was also considered in [16] reporting spectra steeper than k^{-1} in the Batchelor regime. The experimental implementation of the purely additive forcing seems to be difficult from technical point of view and this could be the reason why the Batchelor spectra was never unambiguously observed in laboratory experiments.

Of course, the resetting forcing is an extreme limit. In reality, the relaxation to a certain tracer value cannot be infinitely fast. We expect, however, that similar structures would be observed whenever there is a strong spatial inhomogeneity of the relaxation rate $\alpha(\mathbf{r})$, having values much smaller than the Lyapunov exponent, λ , in some mixing dominated regions and being much larger than λ in others where the relaxational forcing (resetting) would have the main effect.

The 'resetting' model may also be a useful first approximation for chemical tracers in the lower stratosphere. The observed spectra [40], $\gamma \approx 1.8$, fits into the range of our prediction ($1 < \gamma < 2$). Furthermore, cliff-like structures resembling the ones seen in our simple model are characteristic of stratospheric aircraft data. Nonetheless those structures are not separated by smooth regions. The forcing mechanism for stratospheric chemical tracers is likely to be far more complex than that considered here and needs further investigation.

Acknowledgements: The Centre for Atmospheric Science is a joint initiative of the Department of Chemistry and the Department of Applied Mathematics and Theoretical Physics. ZN is supported by the UK Natural Environment Research Council (grant: GR3-12531). GP visited Cambridge with support from Ecole Polytech-

nique, Palaiseau. PH and ZN acknowledge the support of the European Science Foundation in allowing them to attend a Study Centre of the Programme on Transport in Atmospheres and Oceans. Further support for this work came from the EU (through the TOASTE-C programme).

-
- [1] H. Aref, *J. Fluid Mech.* **143** (1984) 1; J. M. Ottino, *The kinematics of mixing: stretching, chaos and transport*, (Cambridge University Press, Cambridge, 1989); A. Crisanti, M. Falcioni, G. Paladin and A. Vulpiani, *Nuovo Cimento*, **14**, 1 (1991)
- [2] J. Chaiken, R. Chevray, M. Tabor and Q. M. Tan, *Proc. Roy. Soc.*, **A408**, 165 (1986)
- [3] W. L. Chain, H. Rising and J. M. Ottino, *J. Fluid Mech.*, **170**, 355 (1986)
- [4] J. C. Sommerer, H. C. Ku and H. E. Gilreath, *Phys. Rev. Lett.*, **77**, 5055 (1996)
- [5] J. M. Ottino, C. W. Leong, H. Rising and P. D. Swanson, *Nature*, **333**, 419 (1988)
- [6] D.W. Waugh, R.A. Plumb, R.J. Atkinson, M.R. Schoeberl, L.R. Lait, P.A. Newman, M. Loewenstein, D.W. Toohey, L.M. Avallone, C.R. Webster, R.D. May, *J. Geophys. Res.*, **99** 1071 (1994).
- [7] R.T. Sutton, H. Maclean, R. Swinbank, A. O'Neill, F.W. Taylor, *J. Atmos. Sci.*, **51**, 2995 (1994).
- [8] K. L. Denman and A. E. Gargett, *Ann. Rev. Fluid Mech.*, **27**, 225 (1995)
- [9] M. G. Balluch and P. H. Haynes, *J. Geophys. Res.*, **102**, 23487 (1997)
- [10] A. F. Tuck and S. J. Hovde, Fractal behavior of ozone wind speed and temperature in the lower troposphere, *Geophys. Res. Lett.* (to appear, 1999)
- [11] G. K. Batchelor, *J. Fluid Mech.*, **5**, 113 (1959)
- [12] A. Vulpiani, *Physica D38*, 372 (1989)
- [13] M. Holzer and E. D. Siggia, *Phys. Fluids*, **6**, 1820 (1994)
- [14] T. M. Antonsen, Z. Fan, E. Ott and E. Garcia-Lopez, *Phys. Fluids*, **8**, 3094 (1996)
- [15] G.-C. Yuan, K. Nam, T. M. Antonsen, E. Ott and P. N. Guzdar, Power spectrum of passive scalars in two-dimensional chaotic flows, preprint (1999)
- [16] P. L. Miller and P. E. Dimotakis, *J. Fluid Mech.*, **308**, 129 (1996)
- [17] B. S. Williams, D. Marteau and J. P. Gollub, *Phys. Fluids*, **9**, 2061 (1997)
- [18] R. T. Pierrehumbert, *Chaos Solitons Fract.*, **4**, 1091 (1993); also in *Chaos Applied to Fluid Mixing*, edited by H. Aref and M. S. El Naschie (Pergamon, 1995)
- [19] E. Zemniak, C. Jung and T. Tél, *Physica D76*, 123 (1994);
- [20] Á Péntek, T. Toroczka, T. Tél, C. Grebogi and J. A. Yorke; *Phys. Rev.*, **E51**, 4076, (1995)
- [21] R. T. Pierrehumbert, *Phys. Fluids*, **A3**, 1250 (1991);
- [22] R. T. Pierrehumbert and H. Yang, *J. Atmos. Sci.*, **50**, 2462 (1993)
- [23] Z. Neufeld, C. Lopez and P. Haynes, *Phys. Rev. Lett.*, **82**, 2606 (1999); Z. Neufeld, C. Lopez, E. Hernandez-Garcia and T. Tél, The multifractal structure of chaotically advected chemical fields, preprint (1999), *chaodyn/9907023*
- [24] M. Chertkov, *Phys. Fluids*, **10**, 3017 (1998); *Phys. Fluids*, **11**, 2257 (1999)
- [25] A. S. Bower, *J. Phys. Oceanogr.*, **21**, 173 (1991)
- [26] E. Ott, *Chaos in dynamical systems*, (Cambridge University Press, 1993)
- [27] C. Grebogi, E. Kosterlich, E. Ott and J. A. Yorke, *Physica* **25D**, 347 (1987)
- [28] S. Bleher, C. Grebogi, E. Ott and R. Brown, *Phys. Rev.* **A38**, 930 (1988)
- [29] T. Tél, 'Transient chaos', in *Directions in Chaos*, Vol. 3, edited by H. Bai-Lin (World Scientific, Singapore, 1991)
- [30] J. D. Farmer, E. Ott and J. A. Yorke, *Physica D7*, 153 (1983);
- [31] G. H. Hsu, E. Ott and C. Grebogi, *Phys. Lett.* **A127**, 199 (1988)
- [32] J. C. Vassilicos and J. C. R. Hunt, *Proc. R. Soc. Lond. A* **435**, 505 (1991)
- [33] R. T. Pierrehumbert, in *Nonlinear Phenomena in Atmospheres and Oceans*, edited by R. Pierrehumbert and G. Carnavale (Springer, New York, 1992)
- [34] T. M. Antonsen, A. Namenson, E. Ott and J. C. Sommerer, *Phys. Rev. Lett.* **75**, 3438 (1995); A. Namenson, T. M. Antonsen and E. Ott, *Phys. Fluids* **8**, 2426 (1996)
- [35] T. Tél, *Zeit. Naturforsch.* **48**, 714 (1982)
- [36] A. S. Monin and A. M. Yaglom, *Statistical Fluid Mechanics* Vol. 2 (MIT Press, Cambridge Mass., 1975)
- [37] H. A. Rose and P. L. Sulem, *J. Physique* **39**, 441 (1978)
- [38] J. C. Sommerer and E. Ott, *Science* **259**, 335 (1993); J. C. Sommerer, *Phys. Fluids* **8**, 2441 (1996)
- [39] K. R. Sreenivasan and R. R. Prasad, *Physica D38*, 322 (1989)
- [40] J. T. Bacmeister, S. D. Eckerman, P. A. Newman, L. Lait, K. R. Chan, M. Loewenstein, M. H. Proffitt and B. L. Gary, *J. Geophys. Res.* **101**, 9441 (1996)

FIG. 1. Stationary tracer field (a) (and blow-up (b)) constructed from 400×400 particles by calculating backwards trajectories until they reach one of the resetting regions. The jet model flow and the parameters used are described in [25]. The forcing domains are, $y > 2.3$ - black and $y < -2.3$ - white. Periodic boundary conditions are used in the x coordinate.

FIG. 2. Stationary tracer distribution (a)(before resetting) using 400×400 particles corresponding to the map (6) using $a = 0.6$ and $\phi = 0$. (b), One-dimensional transect for $x = 0.75$. The resetting domains are stripes parallel to the y axis centered at $x = 0.25$ -black and $x = 0.75$ with width $\epsilon = 0.2$

FIG. 3. Number of iterations needed to reach one of the forcing domains vs. initial coordinates calculated for 2000 points on the line segment shown in Fig. 2b.

FIG. 4. Box counting measurement of the set formed by the discontinuities of the tracer field (calculated with high resolution using 65536 points) measured along three different segments parallel to the x axis $y = 0.1; 0.4; 0.7$. The slope of the power law fit (dashed line) is $D = 0.67$.

FIG. 5. Fractal dimension vs. the width of the forcing stripes ϵ . Dashed line shows the prediction based on (10) and (8), $1 + \ln(1 - 2\epsilon)/\lambda$, using the measured value of the Lyapunov exponent, $\lambda \approx 2.75$.

FIG. 6. Structure functions calculated for three different transects $y = 0.1; 0.4; 0.7$ (a.) and structure function averaged over 10 equidistant transects parallel to the x axis for $\epsilon = 0.2$ (b.). The power law fit (dashed line) has a slope $\zeta = 0.325$.

FIG. 7. The spectral slope γ , vs. the width of the forcing domains, ϵ , based on the measurement of the structure function scaling exponent, ζ , (diamonds), and values predicted from the fractal dimension of the boundary (crosses). The analytical prediction, $1 - \ln(1 - 2\epsilon)/\lambda$, ($\lambda = 2.75$) is also shown (dashed line).

FIG. 8. Tracer distribution (before the resetting) calculated at 400×400 points using the stochastic version of the map (6) with $a = 0.6$ and $\phi_n \in [0, 2\pi]$. The resetting domains are stripes parallel to the y axis centered at $x = 0.25$ -black and $x = 0.75$ with width $\epsilon = 0.2$

FIG. 9. Structure functions for the random case. (a.) Spatially averaged structure functions at 5 different iterations, each calculated by averaging over 10 different transects. ($\epsilon = 0.2$). (b.) Temporal average over spatially averaged structure functions calculated from 10 consecutive iterations. The slope of the power law fit is $\zeta = 0.445$.

This figure "fig1a.png" is available in "png" format from:

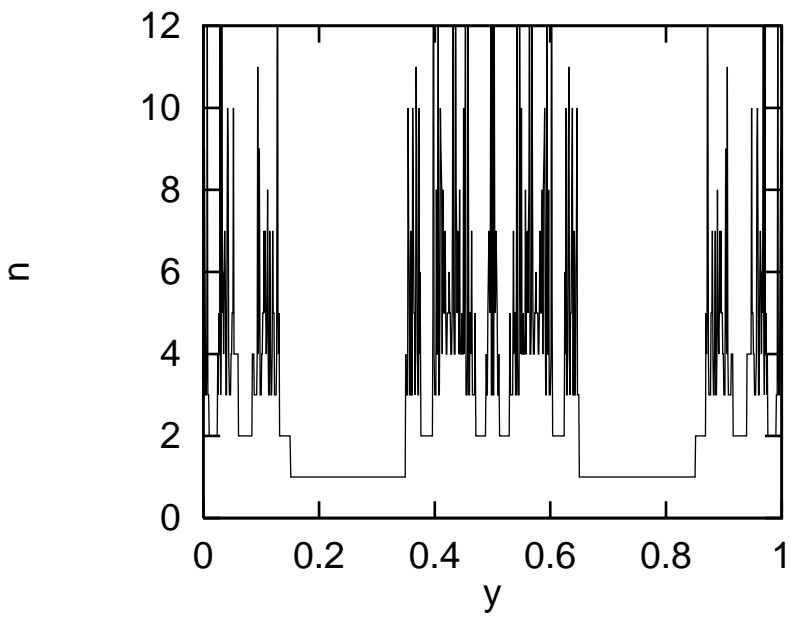
<http://arxiv.org/ps/chao-dyn/9912015v1>

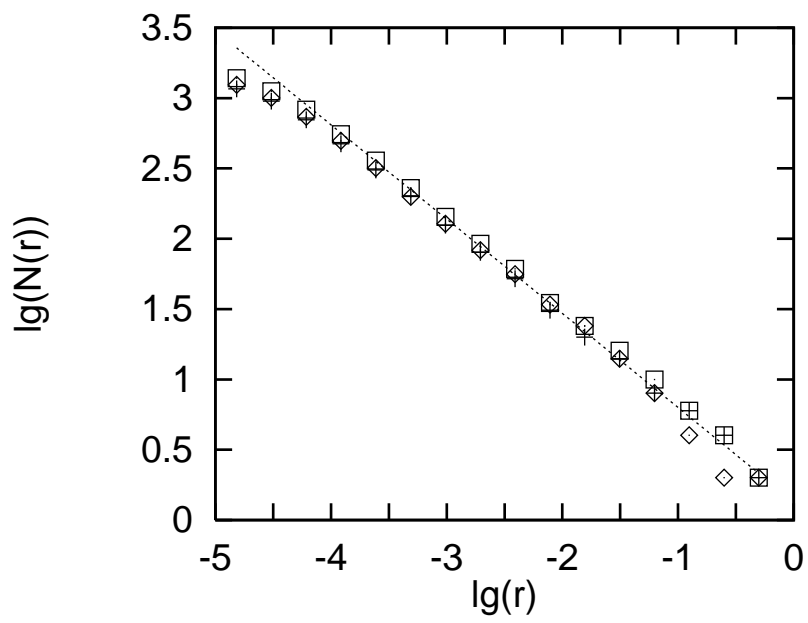
This figure "fig1b.png" is available in "png" format from:

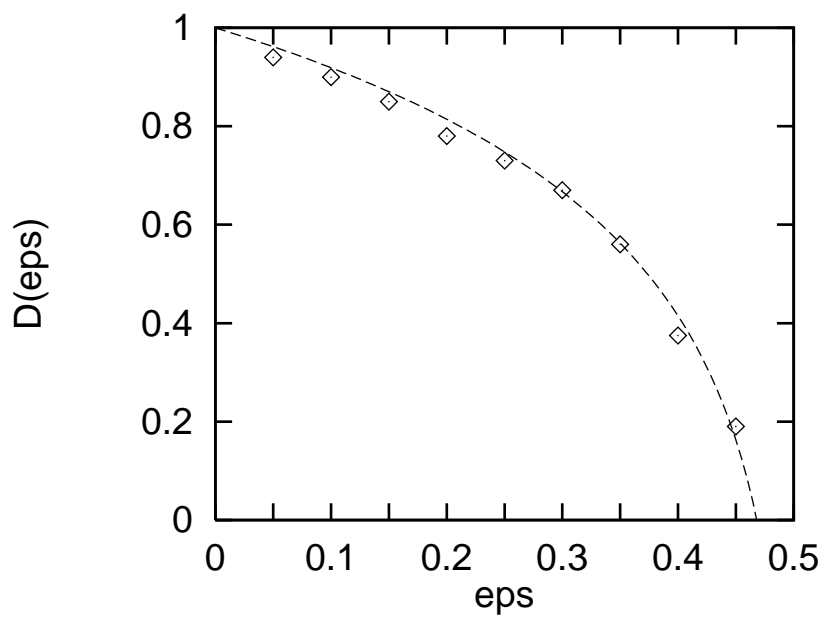
<http://arxiv.org/ps/chao-dyn/9912015v1>

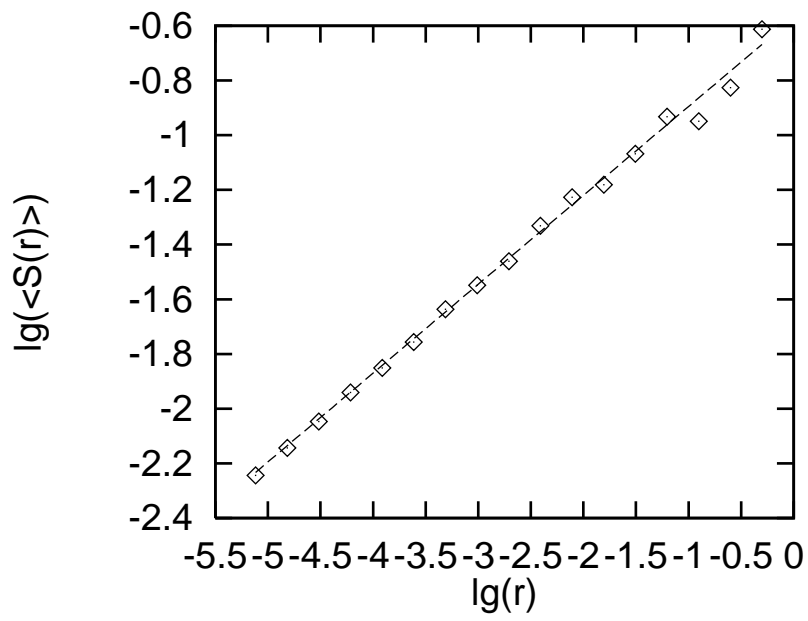
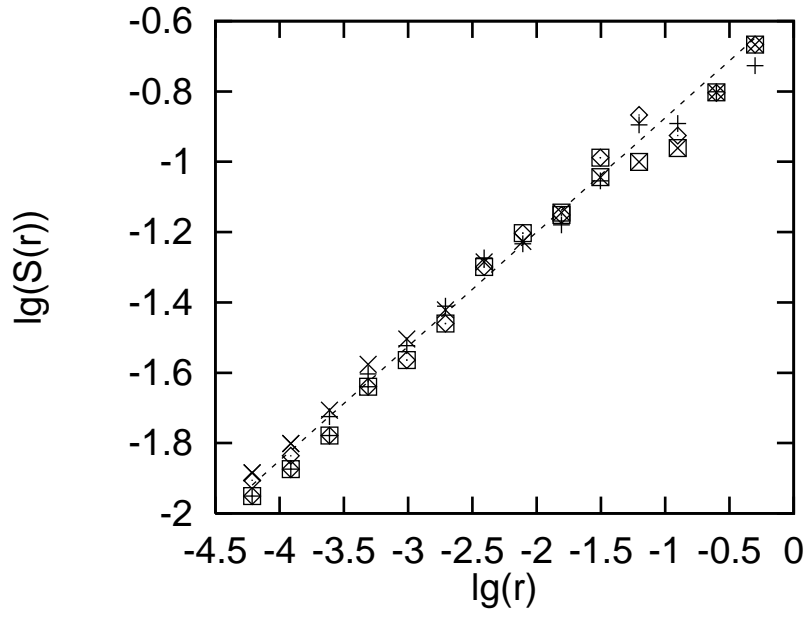
This figure "fig2.png" is available in "png" format from:

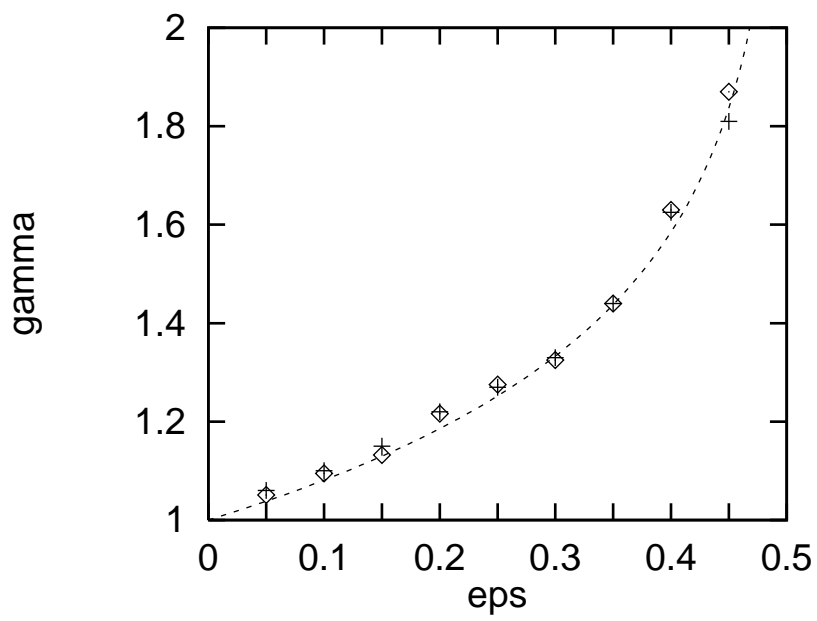
<http://arxiv.org/ps/chao-dyn/9912015v1>











This figure "fig8.png" is available in "png" format from:

<http://arxiv.org/ps/chao-dyn/9912015v1>

